ISSN: 0871-7869

Influence of Modelling Issues on Nonlinear Seismic Analysis of SPEAR Building

A. Belejo; R. Bento

- Novembro de 2012 -

Relatório ICIST
DTC nº 21/2012

LIST OF CONTENTS

1 INTRODUCTION

In the scope of the research project PTDC/ECM/100299/2008 (www.3disp.org), and as far as Task 2 is concerned (evaluate the influence of modelling issues on nonlinear seismic static analysis of 3D irregular structures), some changes in the model of SPEAR building are proposed to take into account some modelling aspects not considered previously (e.g. Bento et al., 2009), aiming the approximation between experimental and analytical results.

The well-known SPEAR building has been tested in terms of seismic behaviour due its plan irregularity. It was built to full-scale and tested within the European project SPEAR (Fardis and Negro, 2006) to represent typical old constructions that do not have any specific provisions for earthquake resistance. It was tested in ELSA lab with a bidirectional loading in three runs of increasing amplitude (0.02g, 0.15g and 0.20g) based on a record obtained in Hercegnovi during 1979 Montenegro earthquake and fitted the EC8 spectrum, type 1 and Soil C (CEN, 2004).

In 2008, in the scope of the International Workshop on Nonlinear Static Methods for Design/Assessment of 3D structures in Lisbon, the seismic assessment of the SPEAR Building (Bento et al., 2009) was performed by means of some nonlinear static procedures and nonlinear dynamic analyses. The model of the SPEAR building considered was validated comparing the numerical results with the experimental ones obtained through the pseudo-dynamically tested (Fardis and Negro, 2006).

The results of top displacements and interstorey drifts obtained over time for an intensity of 0.20g are displayed in Bhatt (2012) and Bento et al. (2009). At that time, the main objective of the work was to compare different type of nonlinear static procedures, and not reproducing completely the experimental behaviour. Therefore, some modelling aspects were not fully considered. Currently, so some changes in the analytical model are performed in order to model the building as close as possible to the one experimentally tested.

2 CASE STUDY – SPEAR BUILDING

The heights of the storeys are 2.75 m for the first floor and 3.00 m for the upper storeys. The building features a non-symmetrical plan configuration but is regular in elevation (Figure 2.1). Only one column (C6) presents a rectangular section of 250×750 mm. All the others have a square cross-section of 250×250 mm. The column C6 and the presence of a balcony on the east side of the structure are the causes for the in-plan irregularity, shifting the centre of mass away from the centre of stiffness, which is very close to the central column (C3).

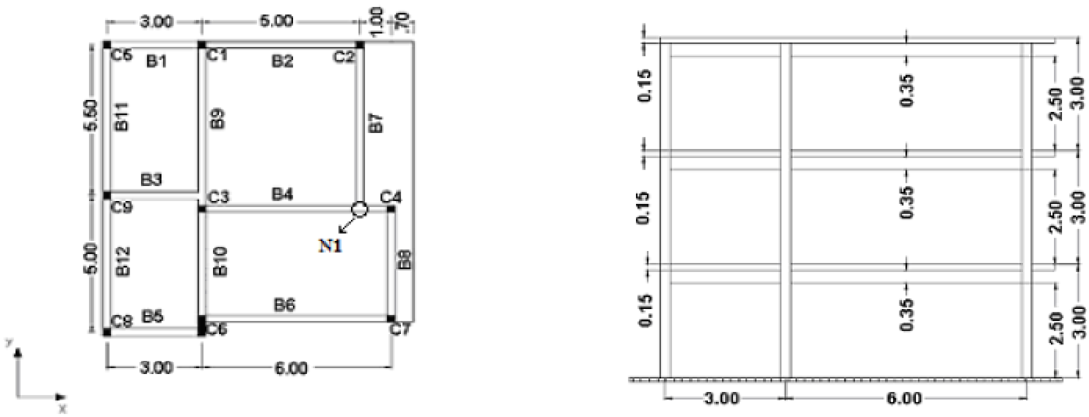

a) b)

Figure 2.1 – SPEAR building: a) Plan view (m); b) Lateral view (m) (Bhatt, 2012)

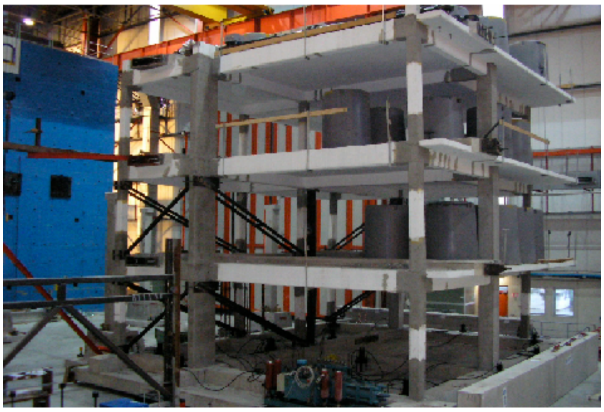

Figure 2.2 – The full-scale SPEAR Building (Fardis et al, 2006)

The concrete is considered unconfined, due to the almost inexistent transversal reinforcement, and a mean compressive strength of 25 MPa was assumed. Average yield strength of 360 MPa and an ultimate strength of 450 MPa were considered for reinforcement steel.

Total translational masses, obtained from the seismic combination, amounted to 67.3 tonnes each for the first two floors and 62.8 tonnes for the roof.

3 MODELLING ISSUES

3.1 Original model

The software used in the modelling of SPEAR building was SeismoStruct (SeismoSoft, 2011) a fibre-based structural program. The building was modelled by an assemblage of inter-connected frame elements using distributed material inelasticity through displacement-based formulation along with geometric nonlinearity.

Each element was discretized into four sub-elements with two integration points each. Fiberized cross-sections − representing sectional details such as cover and core concrete and longitudinal reinforcements − were then defined at respective integration points, whereby every fibre was assigned to an appropriate material constitutive relationship.

The constitutive relationship proposed by Mander et al. (1988) was deployed to model the behaviour of unconfined concrete. In absence of sufficient transverse reinforcement, the confinement effects were not considered for core concrete. The constitutive model used for the steel was proposed by Menegotto and Pinto (1973) including the modifications due to isotropic hardening proposed by Filippou et al. (1983).

A lumped mass modelling strategy was adopted, in which masses were lumped at the nodal points according to its tributary area and by means of the defined masses; the software automatically computed the sustained gravity loads.

The floor slabs of the building possessed very high in-plane stiffness compared to the out-of-plane one; therefore these elements can safely be modelled as ‘rigid diaphragm’. The rigid diaphragm effect was modelled by means of Lagrange Multipliers.

The results displayed in Bhatt (2012) and Bento et al. (2009) in terms of comparison between analytical model and experimental test were obtained considering 0% of damping introduced. However this model issue was reviewed after and a 2% tangent stiffness-proportional damping was introduced to account for possible non-hysteretic sources of damping during analyses.

However some modelling aspects in the work presented in (Bhatt, 2012; Bento et al., 2009) were not considered like beam-column joints, slippage and pullout of smooth reinforced bars, strain penetration length, etc. Thus new modelling features are proposed to take account the most of these aspects to improve the results, taking as reference the experimental results (Fardis and Negro, 2006).

3.2 Modelling changes proposed

Firstly, some changes in the model were applied (one by one) and the results obtained compared with the ones from model used in (Bento et al. 2009) (AN) and the experimental results. Some of the changing options adopted were enabled to improve the results, i.e. minimize the differences between the results of analytical model and experimental test. The ones, which lead to better results, were selected and then combined to obtain the best result possible.

In the following, the different modelling options adopted are described.

3.2.1 Consideration of 2% tangent stiffness-proportional damping (AN_D)

As it was previously mentioned, a 2% tangent stiffness-proportional damping was considered to account for possible non-hysteretic sources of damping during analyses. So for this reason, a 2% tangent stiffness-proportional damping was also introduced.

3.2.2 Elasticity Modulus reduction of Reinforcement Steel (AN_E)

Stiffness reduction of the reinforcement steel is a pragmatic option to consider the slippage and the pullout of smooth reinforced bars (Pinho, 2012); since there is not certain if the reinforcement bars are folded in the ends of the elements. In other hand, ignoring the strain penetration in nonlinear analyses of concrete structures will overestimate the stiffness, hysteretic energy dissipation capacities, strains and section curvature (Zhao and Sritharan, 2007). Therefore to try to overcome these conditionings, the Elasticity Modulus of reinforcement steel is reduced in 25%.

3.2.3 Increase of the Elements' length (AN_L)

The increase of the elements length is an alternative to try to get the nonlinear behaviour for the joints and in other hand to consider the penetration strain length, once ignoring the strain penetration will underestimate the deflections and member elongation. Usually this feature is considered adding this length to the plastic hinge length (Harn et al, 2010). However in this case one are dealing with a fibre-based model where distributed material inelasticity is associated to the elements. For fibre-based elements Ian Zhao and Sri Sritharan (2007) proposed a method which introduces a hysteretic model for the reinforcing bar stress vs. slip response that can be integrated into fibre-based analysis of concrete structures using a zero-length section element, applicable in OpenSEES (PEER, 2006).

This option, of increasing the element length, was applied in two different ways: increasing only 0.10 m the length of each column (AN_L); and increasing 0.10 m the length of the beams connected with external columns (all) and in the last storey columns (AN_L').

3.2.4 Uniform mass distribution (AN_M)

Lumped masses were defined in the columns nodes. To define the masses in each column, the axial forces of a distributed loading were obtained to get the percentage of force in each one. This option was considered because the distribution of water tanks was determined by locating their centre of weight at the centre of weight of slabs (Figure 3.1) to give the same axial force on columns as the uniform load distribution (Jeong and Elnashai, 2005).

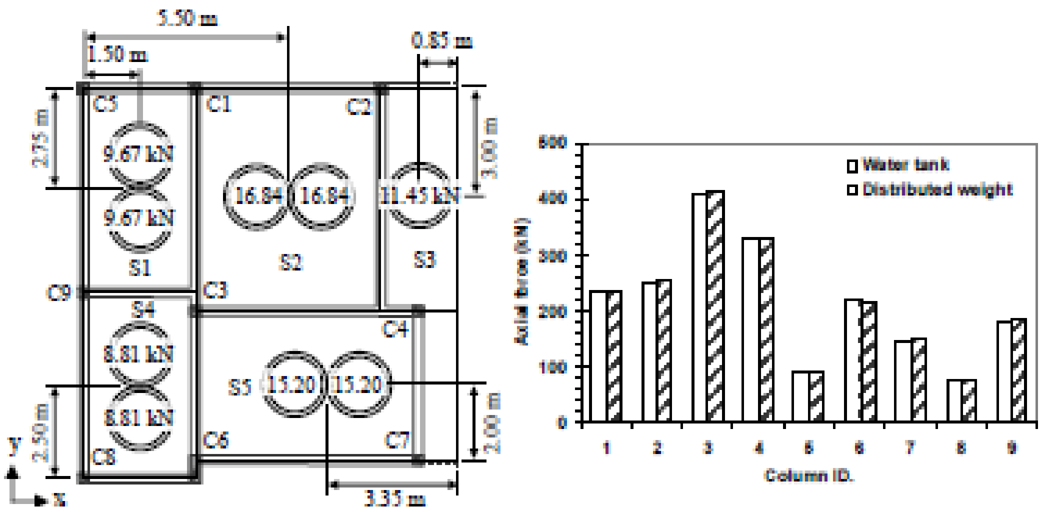

a) b)

Figure 3.1 - Weight determination: (a) Water tank location, (b) Comparison of axial forces on the first story columns between water tank gravity load and uniformly distributed gravity load (Jeong and Elnashai, 2005)

4 COMPARISON OF RESULTS TAKING ACCOUNT ALL PROPOSALS (EXPERIMENT (EXP) VS ANALYTICAL MODEL)

The results herein compared are top displacements and interstorey drifts in nodes C1 and C7 for x direction and nodes N1 and C9 for y direction (Figure 2.1). Also the dynamic characteristics of the structure are compared though knowing that the periods of vibration of the specimen experiment will keep being higher and it is explained due to the reduction of stiffness caused by the cracking in the columns, occurring when the test specimen was transported from outside the ELSA lab, where it was built, into the inside of the laboratory, where it was tested.

For all analytical models, all analyses were performed considering the rigid diaphragm effect modelled by means of Penalty Functions (exponent 10^7) instead of Lagrange Multipliers. Otherwise it would be impractical to perform so many analyses as required.

All the results herein obtained are displayed in percentage, relative to the maximum experimental results. In the following table the maximum results obtained in the experimental test in terms of top displacements and interstorey drifts in x and y direction respectively are shown.

Table 4.1 – Maximum results obtained in the experimental test for x direction

Node	Max Top Displacement	Maximum Interstorey Drift		
		0-1st storey	1st-2nd storey	2nd-3rd storey
C7	114.82 mm	31.6 mm	62.6 mm	34.4 mm
C1	133.08 mm	38.0 mm	72.8 mm	63.6 mm

Table 4.2 - Maximum results obtained in the experimental test for y direction

Node	Max Top Displacement	Maximum Interstorey Drift		
		0-1st storey	1st-2nd storey	2nd-3rd storey
N1	165.17 mm	40.9 mm	80.2 mm	60.2 mm
C9	115.62 mm	30.1 mm	56.8 mm	42.6 mm

4.1 Dynamic Characteristics

In Table 4.3 the first and second periods of vibration of the structure are presented for the alternatives mentioned before. The results presented show that the introduction of stiffness-proportional damping does not cause any difference in the first periods of vibration in the structure. From all the other options, there are small differences, but all of them still far from the values obtained with the experimental specimen, as was expected.

Table 4.3 – First Periods of Vibration of the structure of experimental test and analytical models considering only the change in the models

Case	T1 (s)	T2 (s)
EXP	0.85	0.78
AN	0.62	0.53
AN_D	0.62	0.53
AN_E	0.63	0.53
AN_L	0.65	0.55
AN_L'	0.62	0.55
AN_M	0.62	0.54

Combining these modelling changes, the results obtained are displayed in Table 4.4. In this table are presented the results of the several modelling changes combined: Elasticity Modulus reduction of Reinforcement Steel and Increase of the Elements' length (AN_LE), Elasticity Modulus reduction and Uniform mass distribution (AN_ME), Increase of the Elements' length and Uniform mass distribution (AN_ML) and the combination of these three already mentioned (AN_MLE). Based on these results obtained one can say that by combining all these changes the results get slighter closer to the results from experimental test.

In these combinations, and as far as the increase of elements length concerns, only the increase of the columns was considered. In next sections is shown that this alternative gets equal or better results than the increase of the beams and last storey columns.

Table 4.4 - First Periods of Vibration of the structure of experimental test and analytical models considering combined changes in the models

Case	T1 (s)	T2 (s)
EXP	0.85	0.78
AN	0.62	0.53
AN_LE	0.66	0.56
AN_ME	0.63	0.54
AN_ML	0.66	0.56
AN_MLE	0.66	0.57

4.2 Top Displacements

The top displacements obtained by Bento et al. (2009) for a seismic intensity of 0.20g are displayed in the figures 4.1 and 4.2.

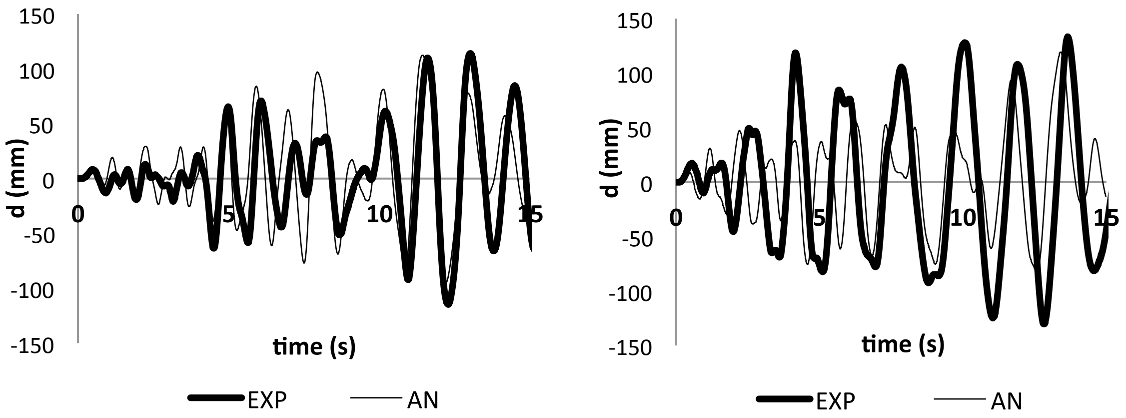

a) b)

Figure 4.1 – **EXP & AN** - Top Displacements in x direction: a) node C7; b) node C1

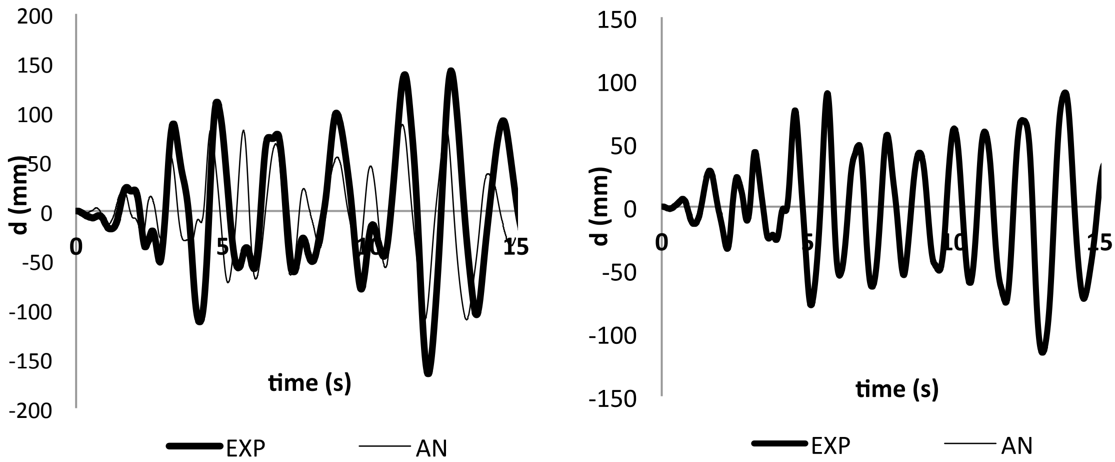

a) b)

Figure 4.2 - **EXP & AN** - Top Displacements in y direction: a) node N1; b) node C9

These displacement profiles, represented with the thin line, should be improved in order to obtain the closest possible to the gross line profiles.

Analysing the different approaches taking account the changes referred one by one, the displacements profiles in the same nodes and corresponding to the same directions are obtained and displayed in the following figures.

Introducing of 2% tangent stiffness-proportional damping

In terms of top displacements, can be seen by Figure 4.3 and Figure 4.4 that the introduction of damping does not improve the results, so all the remaining analyses are made with no damping.

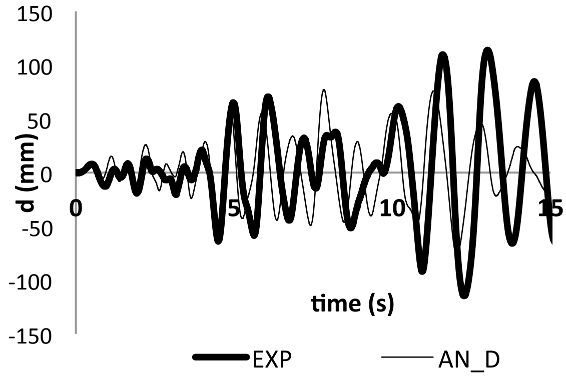

a)

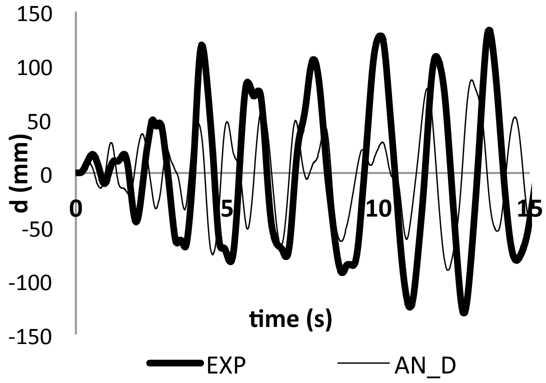

b)

Figure 4.3 - **EXP & AN_D** - Top Displacements in x direction: a) node C7; b) node C1

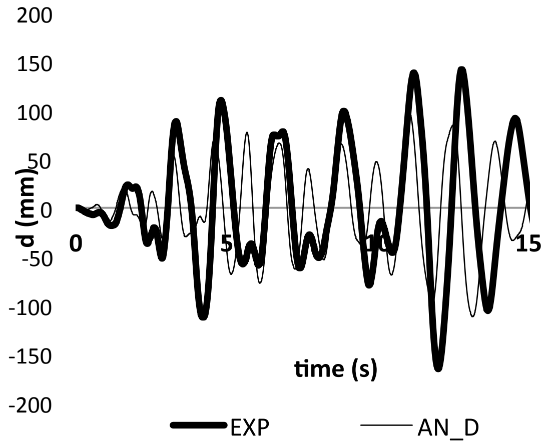

a)

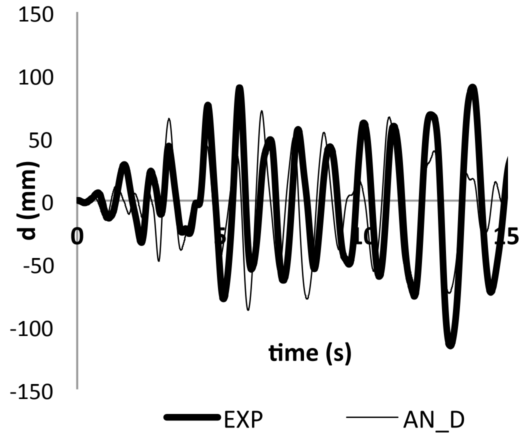

b)

Figure 4.4 - **EXP & AN_D** - Top Displacements in y direction: a) node N1; b) node C9

Elasticity Modulus reduction of Reinforcement Steel

Figure 4.5 and Figure 4.6 depict the results obtained when the elasticity modulus of the reinforcement steel is reduced. Comparing these two figures with Figure 4.1 and Figure 4.2, it is noticed that the top displacements profiles got closer with the referred change in the model, showing almost every cycles with same duration.

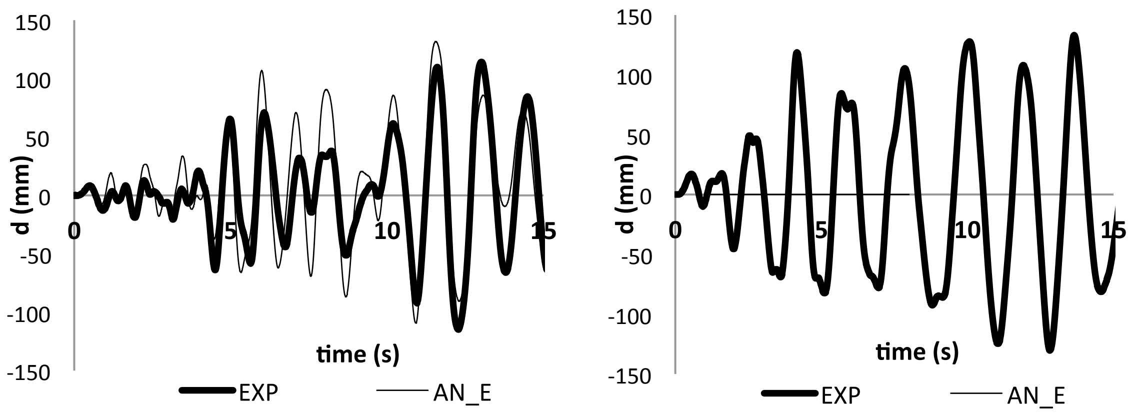

a) b)

Figure 4.5 - **EXP & AN_E** - Top Displacements in x direction: a) node C7; b) node C1

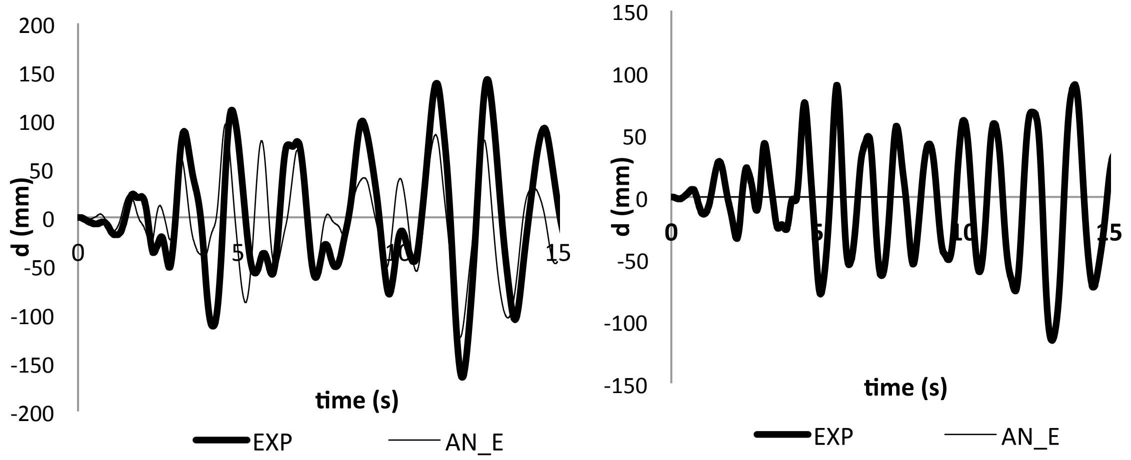

a) b)

Figure 4.6 - **EXP & AN_E** - Top Displacements in y direction: a) node N1; b) node C9

Increase of the Elements' length

The results herein presented show that this option also improves the results. However the differences between the two approaches described are not evident in any case. However in terms of mean and maximum differences, the option that considers only the increase of the length of the columns show better approximation to the experimental test as can be seen in Table 4.5.

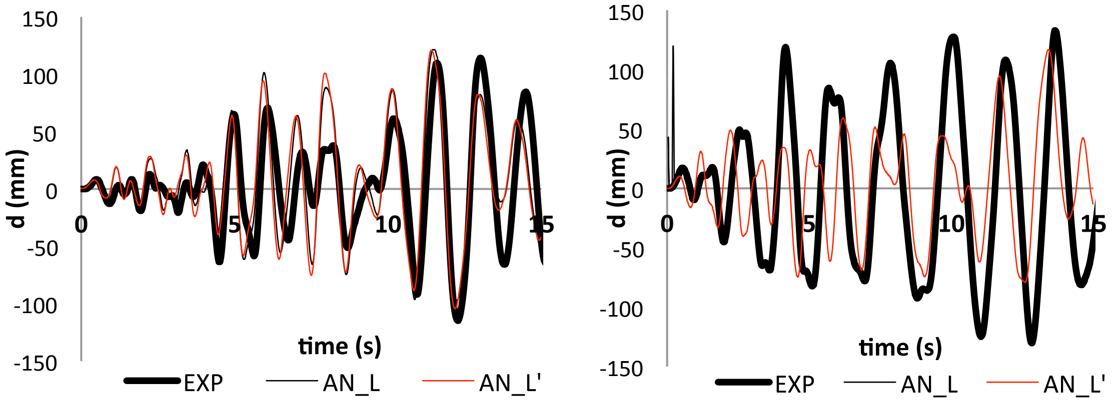

a) b)

Figure 4.7 – **EXP, AN_L & AN_L'** - Top Displacements in x direction: a) node C7; b) node C1

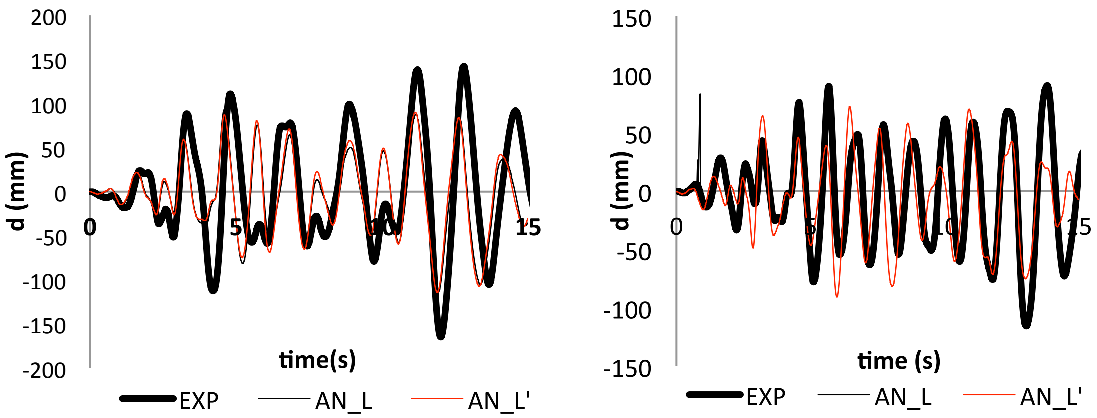

a) b)

Figure 4.8 - **EXP, AN_L & AN_L'** - Top Displacements in y direction: a) node N1; b) node C9

Table 4.5 - Top displacements differences between Experimental test and Analytical models

Case	Mean difference		Maximum difference		Mean difference		Maximum difference	
	x direction				y direction			
	C7	C1	C7	C1	N1	C9	N1	C9
AN	**24%**	**41%**	**71%**	**109%**	**27%**	**26%**	**87%**	**78%**
AN_L	20%	39%	60%	104%	25%	23%	77%	73%
AN_L'	24%	41%	68%	108%	27%	25%	84%	79%

Uniform mass distribution

With the different mass distribution assumed in this study, it is observed that generally the displacements profile has a better match with the experimental test profile.

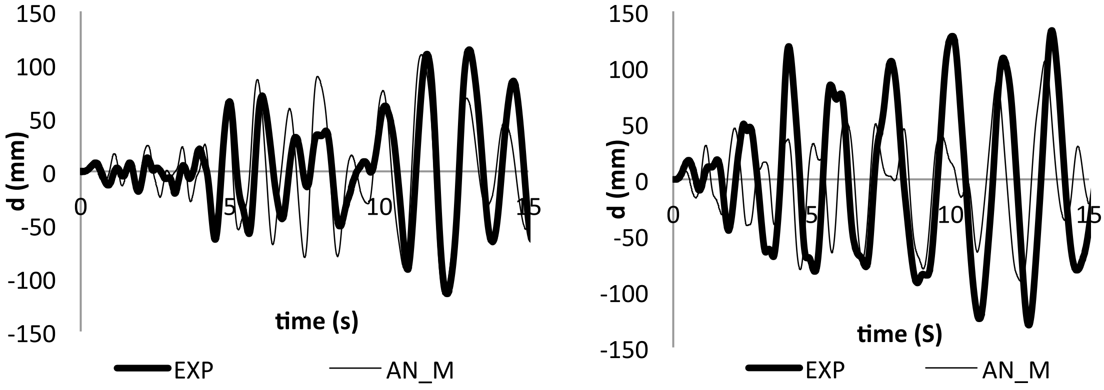

a) b)

Figure 4.9 – **EXP & AN_M** - Top Displacements in x direction: a) node C7; b) node C1

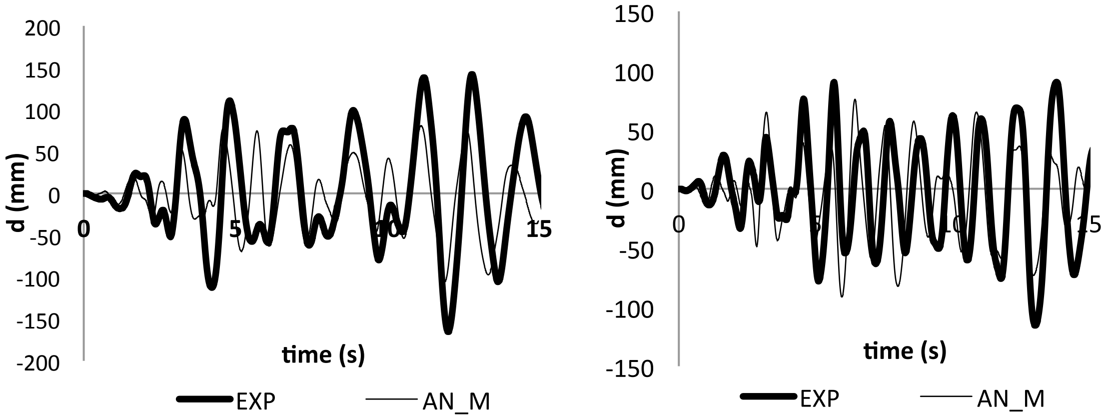

a) b)

Figure 4.10 – **EXP & AN_M** - Top Displacements in y direction: a) node N1; b) node C9

In the following tables there is a summary describing the mean and maximum difference between experimental test and analytical models and still difference between maximum displacements and respective error in the x and y directions respectively.

Table 4.6 –Top displacements differences between Experimental test and Analytical models in x direction

Case	Mean difference		Maximum difference		Difference between maximums	
	C7	C1	C7	C1	C7	C1
AN	**24%**	**41%**	**71%**	**109%**	**-2%**	**-10%**
AN_D	30%	45%	96%	138%	-33%	-32%
AN_E	20%**	38%**	59%**	107%*	13%	-9%*
AN_L	20%*	39%*	60%*	104%**	6%	-8%**
AN_M	24%	41%*	73%	112%	1%**	-21%

* Closer to experimental test results than reference (bold) results
** Closest to experimental test results

Table 4.7 - Top displacements differences between Experimental test and Analytical models in y direction

Case	Mean difference		Maximum difference		Difference between maximums	
	N1	C9	N1	C9	N1	C9
AN	**27%**	**26%**	**87%**	**78%**	**-33%**	**-25%**
AN_D	31%	27%	117%	70%**	-32%*	-38%
AN_E	24%**	23%*	73%**	72%*	-25%**	-1%**
AN_L	25%*	23%**	77%*	73%*	-31%*	-22%*
AN_M	26%*	28%	83%*	83%	-36%	-21%*

* Closer to experimental test results than reference (bold) results

** Closest to experimental test results

From the analysis of the top displacements profiles, Table 4.6 and Table 4.7 show that the changes applied to the model related with stiffness reduction, elements' increase and uniform mass distribution are able to improve the results and obtain closer results to the experimental test comparing to the model used in (Bento et al., 2009).

Therefore the results herein obtained suggest to combine these approaches to get even better match with experimental test.

So, in the following, the top displacements profiles in the same points and for the directions considered previously are shown, combining the different approaches already studied resulting in other four different approaches (the same already used to obtain the first periods of the structure in Chapter 4.1)

Elasticity Modulus reduction of Reinforcement Steel and Increase of the Elements' length

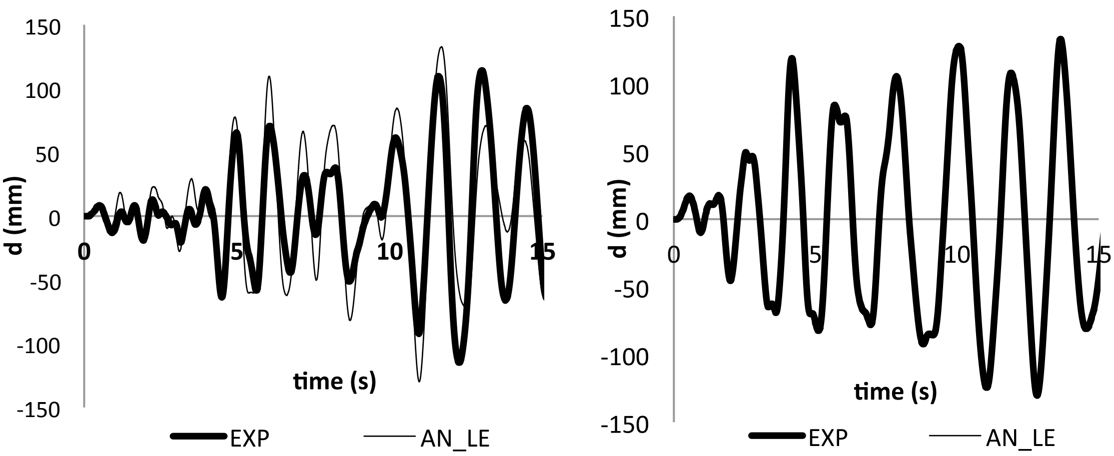

a) b)

Figure 4.11 – **EXP & AN_LE** - Top Displacements in x direction: a) node C7; b) node C1

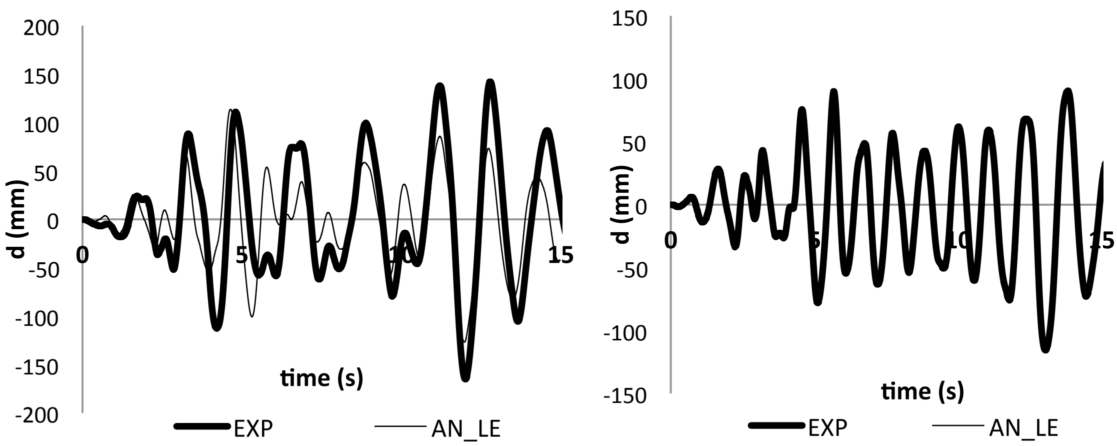

a) b)

Figure 4.12 – **EXP & AN_LE** - Top Displacements in y direction: a) node N1; b) node C9

Elasticity Modulus reduction of Reinforcement Steel and Uniform mass distribution

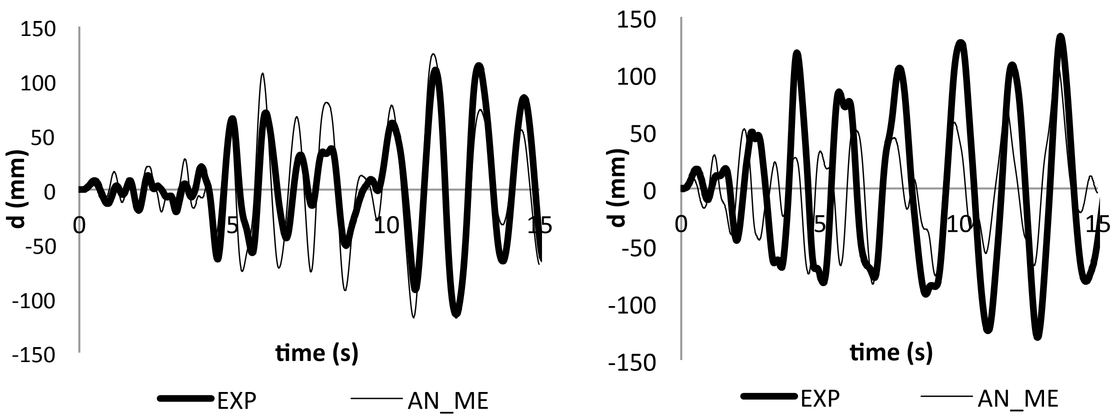

a) b)

Figure 4.13 – **EXP & AN_ME** - Top Displacements in x direction: a) node C7; b) node C1

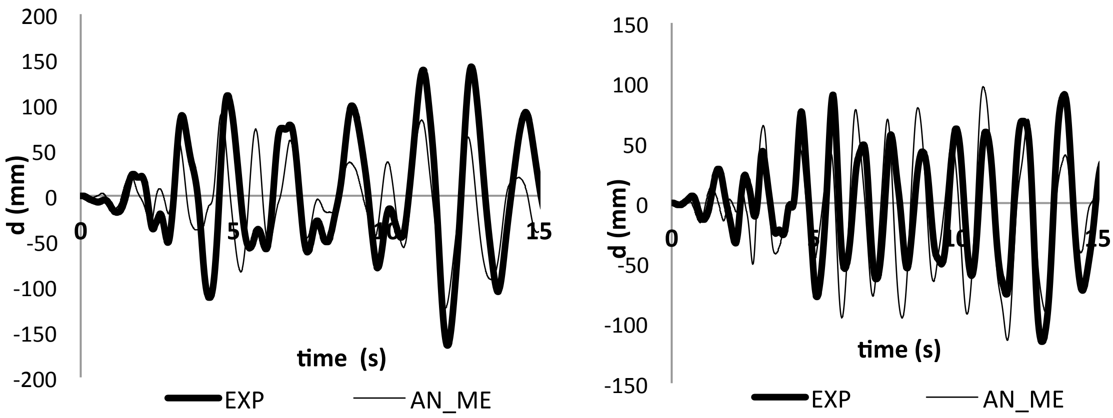

a) b)

Figure 4.14 – **EXP & AN_ME** - Top Displacements in y direction: a) node N1; b) node C9

Increase of the Elements' length and Uniform mass distribution

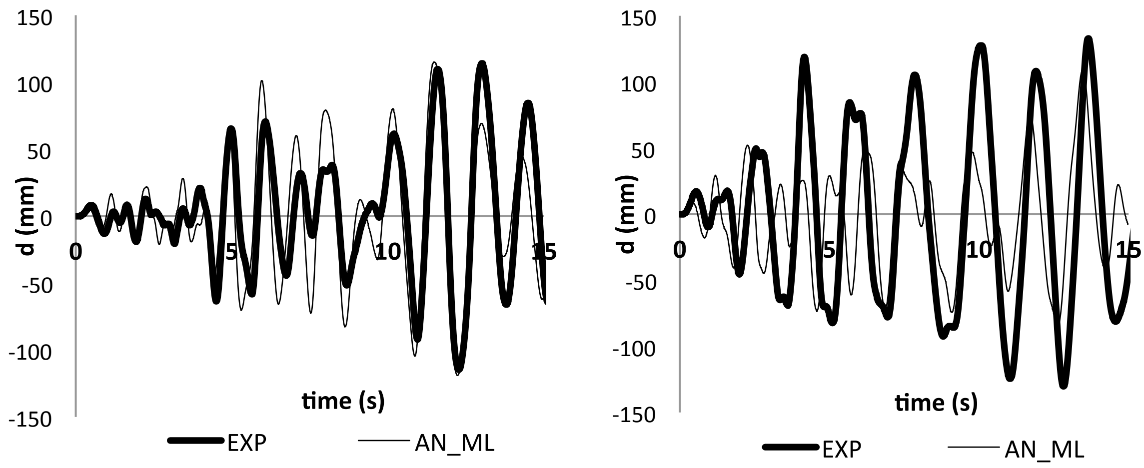

a) b)

Figure 4.15 – **EXP & AN_ML** - Top Displacements in x direction: a) node C7; b) node C1

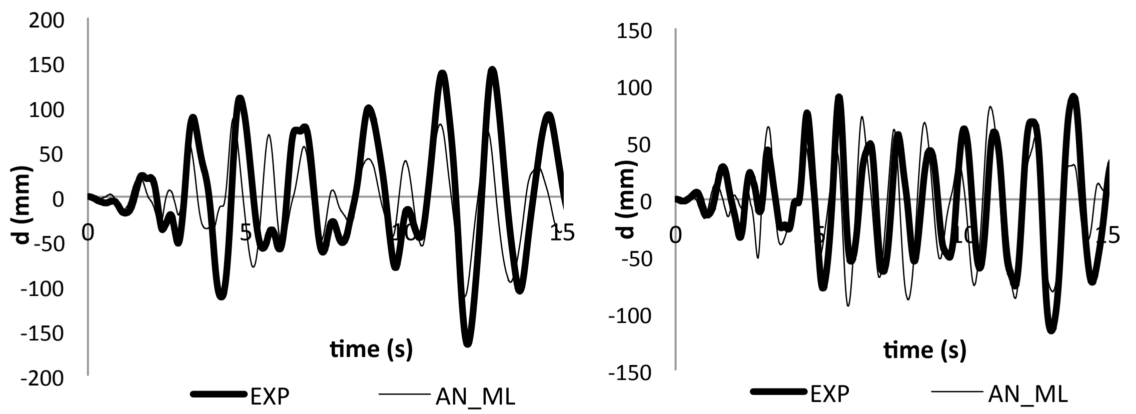

a) b)

Figure 4.16 – **EXP & AN_ML** - Top Displacements in y direction: a) node N1; b) node C9

Elasticity Modulus reduction of Reinforcement Steel, Increase of the Elements' length and Uniform mass distribution

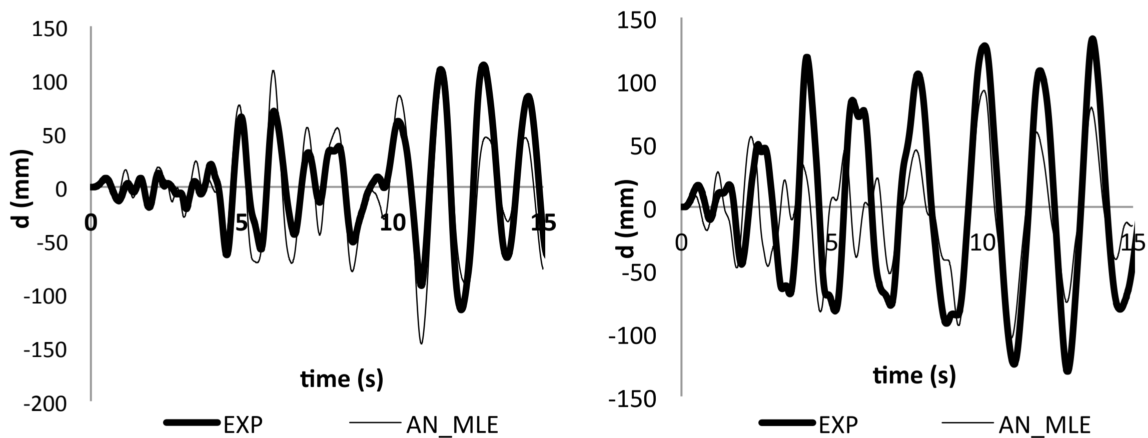

a) b)

Figure 4.17 – **EXP & AN_MLE** - Top Displacements in x direction: a) node C7; b) node C1

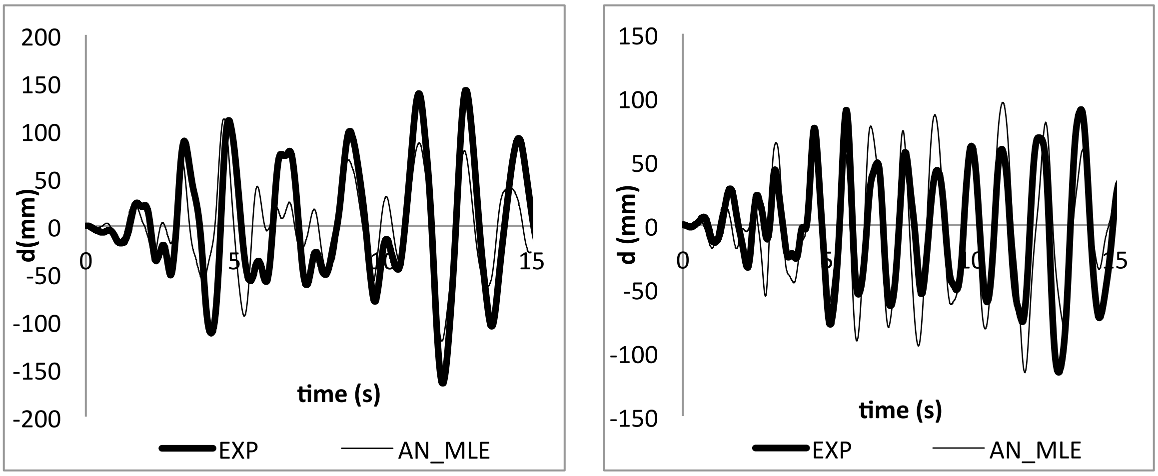

a) b)

Figure 4.18 – **EXP & AN_MLE** - Top Displacements in y direction: a) node N1; b) node C9

The results in terms of differences between experimental test and analytical models are presented in Table 4.8 and Table 4.9. The reference values herein presented, showed in bold, correspond to the minimum values obtained by the approaches, which consider only one change in the model.

Table 4.8 –Top displacements differences between Experimental test and Analytical models in x direction including combined approaches

Case	Mean difference		Maximum difference		Difference between maximums	
	C7	C1	C7	C1	C7	C1
AN	24%	41%	71%	109%	-2%	-10%
AN_D	30%	45%	96%	138%	-33%	-32%
AN_E	**20%**	**38%**	**59%**	107%	13%	-9%
AN_L	20%	39%	60%	**104%**	6%	**-8%**
AN_M	24%	41%	73%	112%	**1%**	-21%
AN_LE	18%**	33%*	56%**	90%*	13%	-28%
AN_ME	19%*	37%*	61%	113%	8%	-18%
AN_ML	20%	39%	65%	108%	22%	-22%
AN_MLE	18%*	30%**	67%	88%**	4%	-18%

* Closer to experimental test results than reference (bold) results
** Closest to experimental test results

Table 4.9 - Top displacements differences between Experimental test and Analytical models in y direction including combined approaches

Case	Mean difference		Maximum difference		Difference between maximums	
	N1	C9	N1	C9	N1	C9
AN	27%	26%	87%	78%	-33%	-25%
AN_D	31%	27%	117%	**70%**	-32%	-38%
AN_E	**24%**	23%	**73%**	72%	**-25%**	**-1%**
AN_L	25%	**23%**	77%	73%	-31%	-22%
AN_M	26%	28%	83%	84%	-36%	-21%
AN_LE	22%*	22%*	64%*	75%	-23%**	9%
AN_ME	24%*	25%	71%*	79%	-25%*	-1%*
AN_ML	25%	25%	77%	79%	-27%	0%**
AN_MLE	21%**	21%**	63%**	65%**	-32%	-19%

* Closer to experimental test results than reference (bold) results
** Closest to experimental test results

Considering these new approaches, where were combined the suggested changes in the models, is verified that the results in terms of top displacements were still improved. The mean difference between top displacements was reduced in some nodes comparing with the “best” results obtained before.

When all changes proposed in the model are combined (except damping addiction), all differences of displacements obtained for both directions are reduced due the good match between top displacements profiles (experimental and analytical). In three nodes, of four analysed, mean and maximum differences are the smallest for this approach.

In Table 4.8 and Table 4.9, the maximum values of the displacements in experimental and analytical analyses are showed, and only in node C7 the analytical test overestimates the displacements for all approaches. In the other nodes top displacements are generally lower compared with experimental test, however with the changes performed in the model, the differences become smaller, getting close to the experimental values.

Interstorey Drifts

To study the structure behaviour of the other stories, also the interstorey drifts were calculated using the analytical model considering the changes mentioned before and the experimental test. So can be verified the influence of the proposed changes in the model for all structure.

The interstorey drifts obtained by Bento et al. (2009) for a seismic intensity of 0.20g are displayed in the Figure 4.19 for the 1^{st}-2^{nd} floor in the x direction and for first floor in y direction for nodes C7 and C9 respectively.

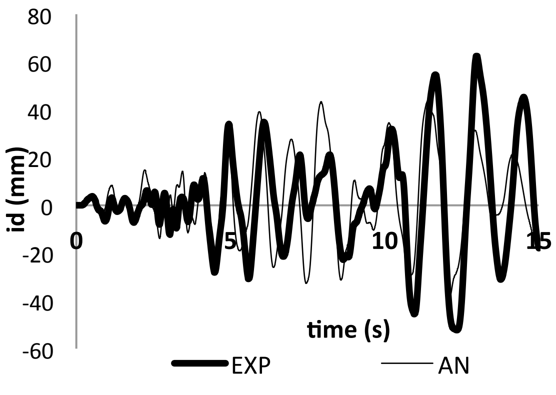

a)

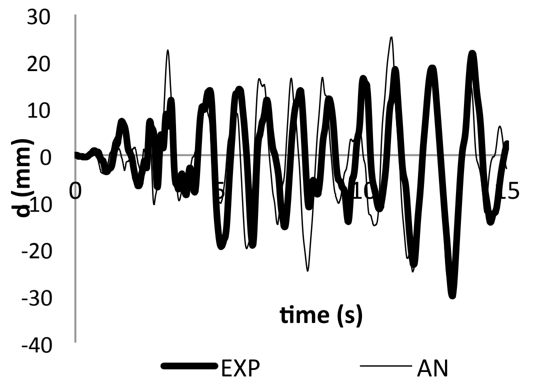

b)

Figure 4.19 – **EXP & AN** – Interstorey drifts: a) 1st storey drifts at node C7 in x direction: a) 1st-2nd stories at node C9 in y direction

The modelling changes, herein considered, are the same, which were applied to obtain the top displacements as well as the combinations performed.

So in the following figures the first floor interstorey drifts in node C9 in y direction and 1st-2nd floors interstorey drifts in node C7 for x direction, are shown considering the referred approaches excluding the model with damping since it shows worst result for top displacements.

Elasticity Modulus reduction of Reinforcement Steel

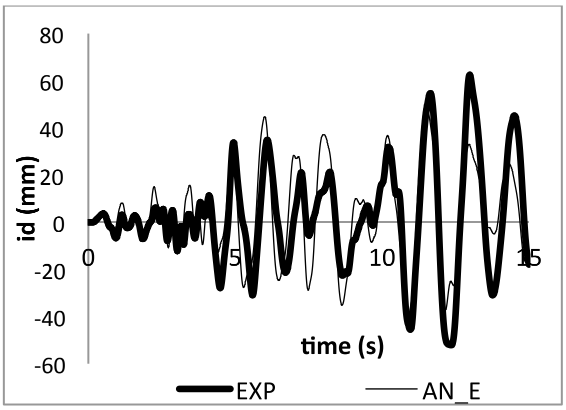

a)

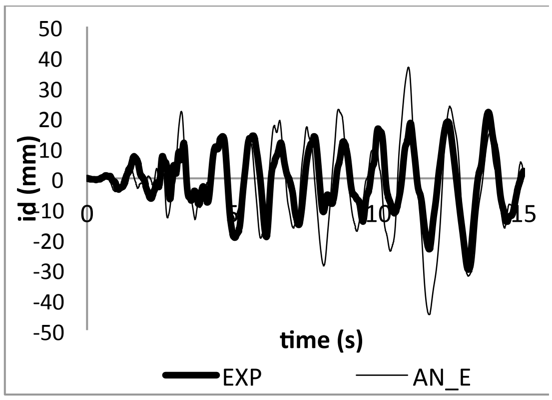

b)

Figure 4.20 – **EXP & AN_E** – Interstorey drifts: a) 1st storey drifts at node C7 in x direction: a) 1st-2nd stories at node C9 in y direction

Increase of the Elements' length

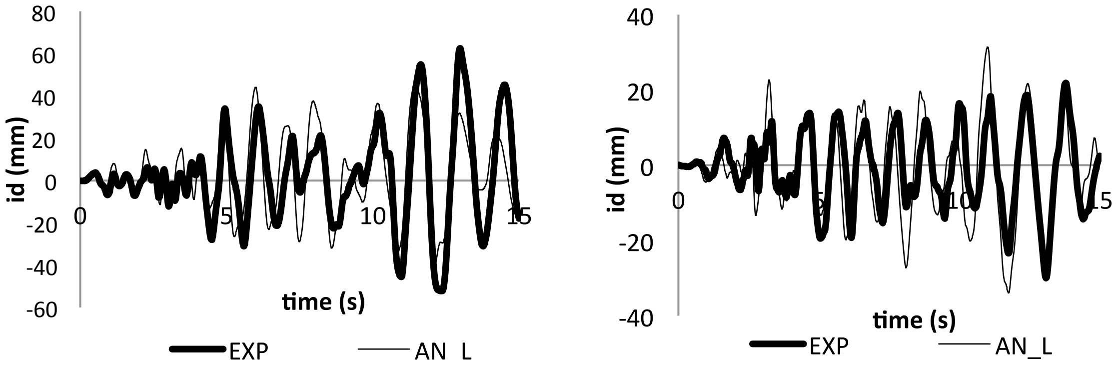

a) b)

Figure 4.21 – **EXP & AN_L** – Interstorey drifts: a) 1st storey drifts at node C7 in x direction: a) 1st-2nd stories at node C9 in y direction

Uniform mass distribution

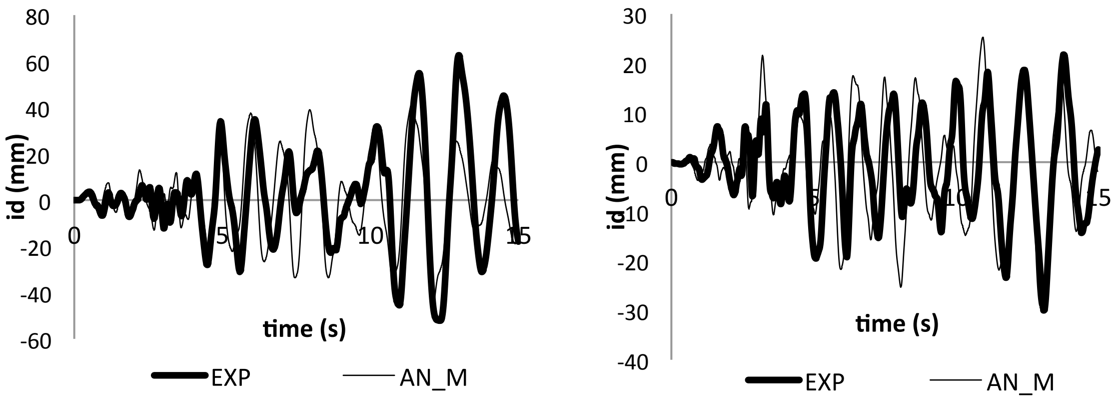

a) b)

Figure 4.22 – **EXP & AN_M** – Interstorey drifts: a) 1st storey drifts at node C7 in x direction: a) 1st-2nd stories at node C9 in y direction

Elasticity Modulus reduction of Reinforcement Steel and Increase of the Elements' length

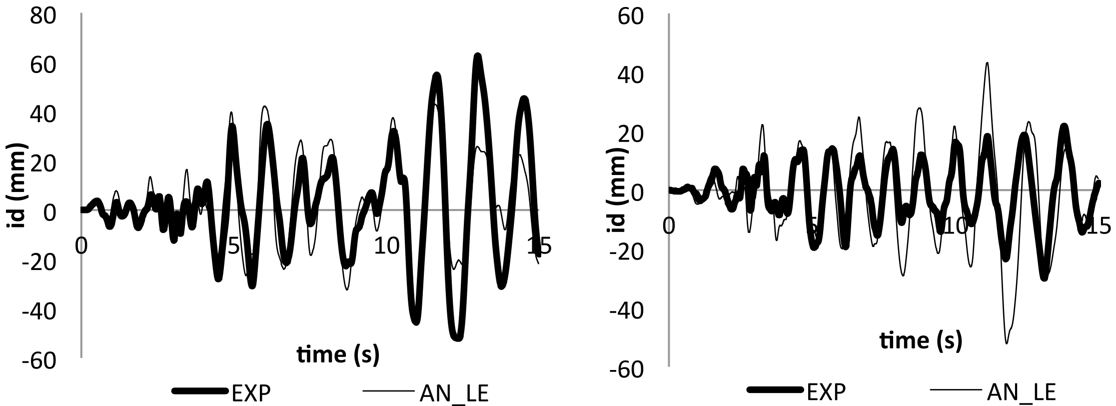

a) b)

Figure 4.23 – EXP & AN_LE – Interstorey drifts: a) 1st storey drifts at node C7 in x direction: a) 1st-2nd stories at node C9 in y direction

Elasticity Modulus reduction of Reinforcement Steel and Uniform mass distribution

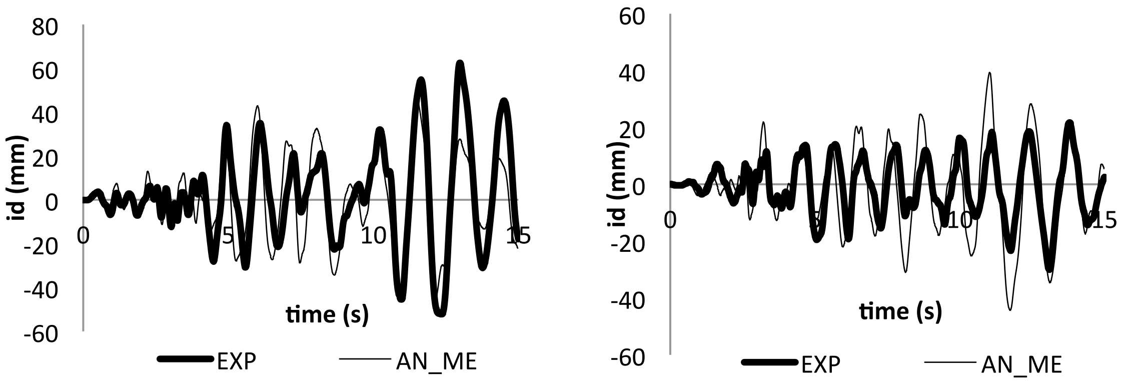

a) b)

Figure 4.24 – **EXP & AN_ME** – Interstorey drifts: a) 1st storey drifts at node C7 in x direction: a) 1st-2nd stories at node C9 in y direction

Increase of the Elements' length and Uniform mass distribution

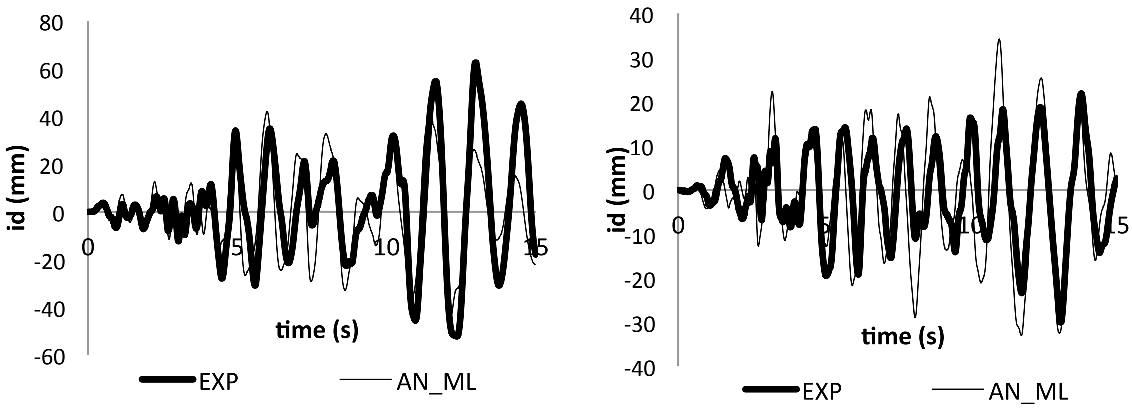

a) b)

Figure 4.25 – **EXP & AN_ML** – Interstorey drifts: a) 1st storey drifts at node C7 in x direction: a) 1st-2nd stories at node C9 in y direction

Elasticity Modulus reduction of Reinforcement Steel, Increase of the Elements' length and Uniform mass distribution

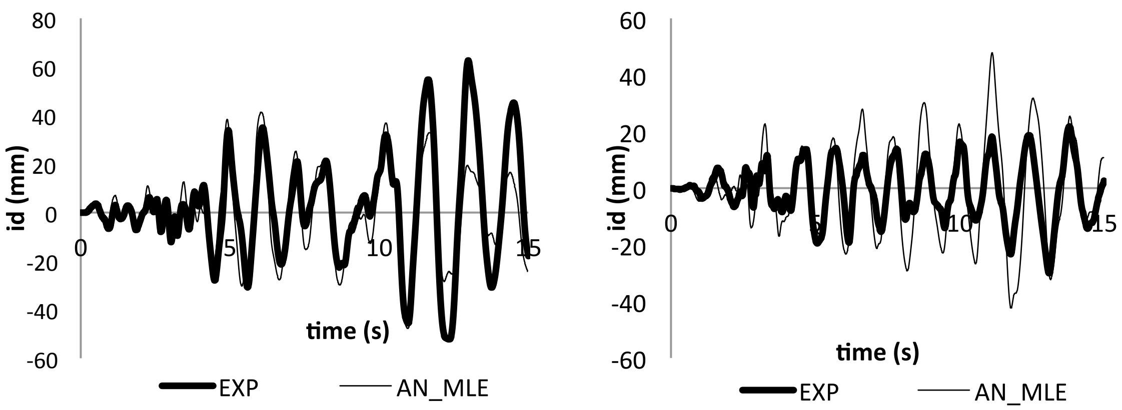

a) b)

Figure 4.26 – **EXP & AN_MLE** – Interstorey drifts: a) 1st storey drifts at node C7 in x direction: a) 1st-2nd stories at node C9 in y direction

From the interstorey drifts profiles, one can conclude that, in most of the cases, there is a very reasonable match between interstorey drifts profiles, improving the results obtained before changing the model. The only exception occurs with the analytical model considering a uniform mass distribution, as can be seen in Figure 4.22.

From the observation of the interstorey drifts profiles can be noticed that for 1st storey the interstorey drifts are overestimated and on other hand, for 1st-2nd storey they are underestimated. However, additional conclusions could be achieved with the observation of Table 4.10 and Table 4.11.

The follow tables show a resume of all interstorey drifts in the four columns considered in each floor (C7 and C1 for x direction and N1 and C9 for y direction).

Table 4.10 – Interstorey Drifts differences between Experimental test and Analytical models in x direction

Case	Stories	Mean difference		Maximum difference		Difference between maximum displacements	
		C7	C1	C7	C1	C7	C1
AN	0-1st	**28%**	**38**%	**104**%	**166**%	**44%**	**-28%**
AN_E	0-1st	30%	36%*	137%	166%	52%	15%*
AN_L	0-1st	28%	36%*	119%	164%*	49%	-11%**
AN_M	0-1st	29%	37%*	107%	143%*	48%	45%
AN_LE	0-1st	32%	29%*	172%	102%**	55%	27%
AN_ME	0-1st	30%	34%*	146%	153%*	55%	48%
AN_ML	0-1st	29%	35%*	119%	141%*	53%	45%
AN_MLE	0-1st	33%	27%**	171%	107%*	52%	19%*
AN	1st – 2nd	**22**%	**34**%	**69**%	**93**%	**-30%**	**-46%**
AN_E	1st – 2nd	18%*	32%*	49%**	77%*	-19%**	-42%*
AN_L	1st – 2nd	19%*	33%*	62%*	84%*	-26%*	-46%*
AN_M	1st – 2nd	22%	34%*	73%	88%*	-27%*	-51%
AN_LE	1st – 2nd	14%*	29%*	59%*	72%*	-28%*	-35%**
AN_ME	1st – 2nd	17%*	32%*	56%*	80%*	-25%*	-51%
AN_ML	1st – 2nd	19%*	33%*	67%*	79%*	-28%*	-53%
AN_MLE	1st – 2nd	14%**	28%**	70%	67%**	-24%*	-45%*
AN	2nd – 3rd	**30**%	**33**%	**97**%	**126**%	**-4%**	**-54%**
AN_E	2nd – 3rd	25%*	32%*	72%*	123%*	16%	-52%*
AN_L	2nd – 3rd	25%*	32%*	78%*	122%*	3%**	-54%
AN_M	2nd – 3rd	30%	34%	100%	129%	-8%	-37%*
AN_LE	2nd – 3rd	20%	30%*	67%*	103%**	17%	-49%*
AN_ME	2nd – 3rd	25%*	32%*	80%*	131%	20%	-31%**
AN_ML	2nd – 3rd	26%*	32%*	81%*	127%	9%	-39%*
AN_MLE	2nd – 3rd	19%**	30%**	63%**	103%*	15%	-44%*

* Closer to experimental test results than reference (bold) results
** Closest to experimental test results

Table 4.11 - Interstorey Drifts differences between Experimental test and Analytical models in y direction

Case	Stories	Mean difference		Maximum difference		Difference between maximum displacements	
		N1	C9	N1	C9	N1	C9
AN		**26%**	**23**%	**113**%	**83**%	**29%**	**62%**
AN_E		25%*	25%	109%*	80%*	30%	62%*
AN_L		25%*	23%**	101%*	78%**	27%*	61%*
AN_M	0-1st	25%*	25%	99%*	90%*	21%*	-2%**
AN_LE		22%*	27%	87 %*	131%*	26%*	44%*
AN_ME		25%*	27%	103%*	87%*	32%	32%*
AN_ML		24%*	25%	92%*	86%*	25%*	12%*
AN_MLE		19%**	27%	83%**	100%*	9%**	37%*
AN		**25**%	**24**%	**87**%	**72**%	**-52%**	**-41%**
AN_E		23%*	21%*	70%*	63%**	-49%*	-43%
AN_L		24%*	21%*	81%*	66%*	-50%*	-45%
AN_M	1st – 2nd	25%*	25%	87%*	76%	-56%	-29%*
AN_LE		21%*	20%*	58%*	76%	-36%**	-36%*
AN_ME		24%*	22%*	72%*	65%*	-50%*	-25%*
AN_ML		24%*	22%*	81%*	68%*	-52%*	-28%*
AN_MLE		21%**	19%**	58%**	70%*	-37%*	-21%**
AN		**30**%	**26**%	**100**%	**90**%	**-33%**	**-4%**
AN_E		28%*	22%*	92%*	80%*	-25%*	-6%
AN_L		28%*	23%*	90%*	78%*	-26%*	-11%
AN_M	2nd – 3rd	29%*	27%	97%*	91%	-36%	-26%
AN_LE		26%**	19%**	83%*	79%*	-23%**	-14%
AN_ME		28%*	24%*	90%*	86%*	-27%*	-18%
AN_ML		28%*	25%*	92%*	82%*	-29%*	-22%
AN_MLE		26%*	19%*	79%**	75%**	-28%*	-21%

* Closer to experimental test results than reference (bold) results
** Closest to experimental test results

Based on the values presented Table 4.10 and Table 4.11, one can conclude that the approach which considers uniform distribution of mass also leads to worst results in terms of mean differences, however does not present significant differences. The same conclusion can be stated for the approaches that the uniform mass distribution is combined with other changes in the model. Nevertheless the approach that considers the three changes in model (i.e. uniform mass distribution, Elasticity Modulus reduction of Reinforcement Steel and increase of the elements' length) generally shows the best results. The other approaches that does not consider the uniform mass distribution, generally present improved results.

In terms of maximum displacements, all analytical models show different behaviour comparing with the results from the experimental test. Although the differences between experimental and analytical results had been reduced, the analytical models present the highest interstorey drifts in the first floor, i.e. they overestimate the results. In the other hand, the results from experimental test show the 1^{st}-2^{nd}-storey drift as the highest and for this case analytical models lead to underestimated results. The same occurs in 2^{nd}-3^{rd} interstorey drift, nevertheless with much smaller differences. It means that in 2^{nd} and 3^{rd} floor, the analytical models are not being able to pick up to model what has been occurred in the experimental test. The reason can be related with the damage in some local areas (columns, joints, etc.) of the structure, which could be occurred when the test specimen was transported from outside the ELSA lab, into the inside of the laboratory, as previously mentioned.

5 CONCLUSIONS

The conclusions of this study are described having as reference, the experimental test performed with a record obtained in Hercegnovi during 1979 Montenegro earthquake fitted to EC8 spectrum (type 1 and soil C) considering a peak ground acceleration of 0.20g.

Five different changes in the original analytical model, previously explained, were performed to take in account some modelling aspects not considered before. Into these five changes, two of them were excluded based on the top displacements results obtained only with these individual changes: 1- Introduction of damping and 2- increase of the length of the beams and last storey columns. The analytical results considering the damping in the model showed the worst results in terms of profiles matching and mean and maximum differences, when compared with experimental test. The analytical model considering increase of the length of the beams and last storey columns presented worst results when comparing with the one, which all columns were increased. Thus, since both analytical models were performed to consider the same aspects, only one was chosen to continue the study.

After excluded the two abovementioned models, the study continued with the analytical models remained; they were combined becoming four more different analytical cases (considering uniform mass distribution and elasticity modulus reduction, uniform mass distribution and increase of columns length; elasticity modulus reduction and increase of columns length and the three changes in the same model). Observing the top displacements results obtained from the combined approaches it was verified that they are even better in terms of profiles and mean and maximum differences. And the approach, which is closer to the experimental test results, is the one considering the three changes simultaneously in the analytical model. The same conclusions had already been taken, though with less significance, when the first periods of vibration obtained were compared. In terms of maximum displacements, the changes in the model were able to approximate the results to the results of the experimental test in same nodes. However there is not a total agreement in the results between approaches, nodes or directions in this study, i.e. it is not possible to identify a final model which leads to better results, for all type of outcomes analysed.

As far as interstorey drifts concern, the results were obtained taking into account all the analytical models, considering the modelling changes individually and combined, as previously mentioned. The change performed, in the analytical models, related with mass distribution does not have much influence in the interstorey drifts results. In opposite the other changes have significant importance, yielding to a very reasonable match between experimental test and analytical models interstorey drifts. Similarly, the results related with mean and maximum differences were improved due these changes.

The analytical models are not getting the interstorey drifts obtained in the experimental test, even showing soft storey problems in different storeys.

Taking in account the set of differences performed in the model, it is difficult to get closer than the results herein presented given that the conditions of the experimental specimen are not known in detail.

To conclude, the changes performed in the model to decrease the stiffness of the model, to increase the elements and to have exactly the same distribution of mass presented in the test are reasonable and valid choices to overcome the modelling problems described in this study, which usually are not taking in account for seismic studies, though in some cases may be relevant.

ACKNOWLEDGMENTS

The authors would like to acknowledge the financial support of the Portuguese Foundation for Science and Technology through the research project PTDC/ECM/100299/2008.

REFERENCES

Bento, R. Pinho. (2009). 3D Pushover 2008 – Nonlinear Static Methods for Design Assessment of 3D Structures. IST Press, http://www.3dpushover.org/

Bhatt C. (2012) Seismic Assessment of Existing Buildings Using Nonlinear Static Procedures (NSPs) - A New 3D Pushover Procedure; Thesis specifically prepared to obtain the PhD Degree in Civil Engineering; Technical University of Lisbon

CEN, Eurocode 8 (EC8) 2004: Design of structures for earthquake resistance. Part 1: general rules, seismic actions and rules for buildings. EN 1998-1:2004 Comité Européen de Normalisation, Brussels, Belgium.

Fardis M. N. and Negro P. (2006): SPEAR – Seismic performance assessment and rehabilitation of existing buildings, Proceedings of the International Workshop on the SPEAR Project, Ispra, Italy.

Filippou, F.C., Popov, E.P. and Bertero, V.V. (1983). Modelling of R/C joints under cyclic excitations. *J. Struct.Eng.* **109(11)**, 2666-2684

Harn, Robert E., Mays, Timothy W. and Johnson Gayle S. (2010) - Proposed Seismic Detailing Criteria for Piers and Wharves. Proceedings of Ports 2010: Building on the Past, Respecting the Future.

Jeong S. H. and Elnashai A. S., (2005). Analytical assessment of a 3D full scale RC building test. Proceedings of the International Workshop on the SPEAR Project, Ispra, Italy

Mander JB, Priestley MJN, Park R (1988) Theoretical stress–strain model for confined concrete. *ASCE J Struct Eng* **114(8),** 1804–1826.

Menegotto M. and Pinto P.E. (1973). Method of analysis for cyclically loaded RC plane frames including changes in geometry and non-elastic behaviour of elements under combined normal force and bending. International Association for Bridge and Structural Engineering, Symposium on the Resistance and Ultimate Deformability of Structures anted on by well defined loads, 15-22. Zurich, Switzerland

PEER, 2006 OpenSEES: Open System for Earthquake Engineering Simulation. Pacific Earthquake Engineering Research Center, University of California, Berkeley, CA.

Pinho R, (2012) - Modelação Sísmica de Edifícios Irregulares B.A – Alguns Aspectos Críticos Curso de Formação "Análise Estáticas Não Lineares (Análises Pushover) para o dimensionamento e avaliação sísmica de estruturas". Slides, FUNDEC, IST, Lisbon, Portugal

SeismoSoft, 2011, "SeismoStruct – A computer program for static and dynamic nonlinear analysis of framed structures" available online from http://www.seismosoft.com.

Zhao, J., and S. Sritharan. (2007) - Modelling of strain penetration effects in fiber-based analysis of reinforced concrete structures. ACI Structural Journal, 104(2), pp. 133-141